ARTICLE

Gelled Ionic Liquid/PMMA Polymer Electrolyte Prepared by Radical Polymerization

Li-bo Li[a*], Shuo Yang[a], Jie-si Li[a], Shao-wen Guo[b]

a. Key Laboratory of Green Chemical Engineering and Technology of College of Heilongjiang Province, College of Chemical and Environmental Engineering, Harbin University of Science and Technology, Harbin 150040, China

b. Department of Electro-Machanical Control and Automation, Heilongjiang Institute of Technology, Harbin 150050, China

(Dated: Received on February 20, 2014; Accepted on April 28, 2014)

The gel polymer electrolyte containing *N*-propyl, methylpyrrolidinium bis((trifluoromethyl) sulfonyl)imide (PYR13TFSI) with better performance is prepared by radical polymerization method. The interface status between the $LiFePO_4$ electrode and the electrolyte is characterized by a scanning electron microscope and X-ray photoelectron spectroscopy (XPS). There is a layer of membrane on the gel electrolyte and perfect shell membranes on the surface of active $LiFePO_4$ cluster, on the other hand, N and S photoelectron signals are observed in XPS spectra after charge-discharge cycles. The results show that the ionic liquids and unpolymerized methyl methacrylate incorporate into the electrode surface and form the SEI membrane with Li ion and electrons while the gel electrolyte contacts with the electrode. The formation process of the SEI membrane needs at least three cycles, the discharge capacity increases as the SEI membrane becomes sufficiently thick, which blocks further electron transfer, and the system may approach steady state. The performance of cell with ionic liquid gel polymer electrolyte is measured at different rate. The cells retain 132 mAh/g at 0.2 C, 128 mAh/g at 0.5 C, and 120 mAh/g at 1.0 C after 30 cycles with charge-discharge efficiency of ca. 98% at every rate.

Key words: Radical polymerization, Gelled, Electrolyte, Electrochemistry

I. INTRODUCTION

Since the development of the first rechargeable lithium-ion battery in 1991, lithium-ion (Li-ion) batteries have become the state-of-the-art, rechargeable, compact energy-storage system not only for portable consumer electronics, but also for hybrid electric vehicles (HEVs), and for the storage of electrical energy from fluctuating sources like wind and solar energy [1, 2]. However, due to the high reactivity of Li, Li ion battery has a disadvantage from a view-point of safety, *i.e.*, flammable, overcharging, and also insufficient cycle stability [3]. In the advancement of the lithium battery technology, it is expected to replace the common liquid electrolyte by a highly conducting polymer membrane. Indeed, gel polymer electrolyte rechargeable lithium batteries are promising systems to overcome the performance of conventional liquid electrolyte systems [4−7]. On the other hand, room temperature ionic liquids (RTILs), which are entirely composed of ions, currently attract considerable attention as potentially benign solvents for many areas of electrochemical devices such as rechargeable lithium batteries, fuel cells, electrochemical capacitors, and photoelectrochemical cells. This interest is mainly driven by the alternative features of ionic liquids to traditional organic solvents and electrolytes, such as nonvolatility, nonflammability, electrochemical and thermal stabilities, and high ionic conductivity. Among them, a special fascination of the ionic liquids, especially in materials science field, is that their fluidity and ionic conductivity can be tailored by the selection of both cation and anion components [8, 9]. Therefore, RTILs are considered to be suitable electrolyte salts for polymer-in-salt system.

Ionic liquids meet the requirements of plasticizing salts and offer improved thermal and mechanical properties to flexible polymers. Different polymer electrolytes containing RTILs including ionic liquid-polyelectrolyte systems and gel polymer electrolytes containing hydrophilic and hydrophobic ionic liquids have been reported to possess high conductivity, which is suitable for applications [10−18].

During charge and discharge, lithium ions migrate between two electrodes through the electrolyte and react

*Author to whom correspondence should be addressed. E-mail: llbo2002@126.com, Tel.: +86-451-86392713, FAX: +86-451-86392708

with the electrode materials. Details of these reactions and their consequences are critical to the performance and reliability of batteries [2]. In cells with liquid electrolytes, favorable electrode-electrolyte interfaces are formed merely by soaking electrodes in liquid electrolytes; in cells with solid electrolytes, electrode and electrolyte powders are intentionally contacted to form close solid-solid interfaces [19]. In this work, we research on the composition and the status of the electrode-electrolyte interface membrane, and further, present a model of interfacial status between ionic liquid gel polymer electrolyte and electrode for lithium ion batteries.

II. EXPERIMENTS

A. Preparation of PYR13TFSI

N-propyl, methylpyrrolidinium bis((trifluoromethyl) sulfonyl)imide (PYR13TFSI) was prepared by anion exchange reaction from Br^- to $TFSI^-$ which was carried out by mixing two aqueous solutions of equimolar *N*-propyl, methylpyrrolidinium bromide (PYR13Br) and lithium bis(trifluoromethanesulfonyl)imide (LiTFSI) at room temperature for 24 h to be phase-separated into hydrophobic ionic liquid and aqueous phases.

B. Preparation of polymer electrolytes containing ionic liquids

Polymer electrolyte containing PYR13TFSI was prepared by radical polymerization. Firstly, the methyl methacrylate (MMA) was prepolymerized by heating the solutions at 90 °C for 10 min in water bath in the presence of 0.6wt% benzoyl peroxide (BPO) as an initiator. Secondly, the prepolymer, LiTFSI and ethylene glycol dimethacrylate (EGDMA) with a weight ratio of 20:20:1 were mixed and stirred vigorously for 24 h, and then put into vacuum oven at 80 °C for 16 h. Finally, the flexible polymer electrolyte membranes were obtained and stored in a glove box under argon atmosphere.

C. Preparation of $LiFePO_4$ electrode

In cell, the $LiFePO_4$ mixture as cathode contained active material powder, acetylene black and poly(vinylidene fluoride) (PVdF) binder (10wt% PVdF which was dissolved in *N*-methyl pyrrolidone (NMP) solvent) with a weight ratio of 8:1:1. The viscous black slurry was coated onto the aluminum foil and dried at 100 °C under vacuum for 24 h, then pressed at the pressure of 10 MPa, and finally, cut into 14 mm diameter cathode discs for use as the cathode.

D. Membranes characterization

Surface morphology was investigated by using a Philips FEI Sirion scanning electron microscopy (SEM), and the accelerating voltage of the SEM was 20 kV. X-ray photoelectron spectroscopy (XPS, PHI-5700, ESCA System) with an Al Kα X-ray source (1486.6 eV) at 45° take-off angle was used to analyze the surface electronic states, the pass energy used to record the wide scan XPS spectra was 187.85 eV and the pass energy was 29.35 eV for high resolution scans. All XPS peaks were referenced to the C1s signal at a binding energy of 284.6 eV. Thermal analysis of the electrolyte membranes was carried out using thermogravimetry/differential thermal analyzer (TGA/SDTA851, Swiss Mettler Company) with a heating rate of 10 °C/min over the temperature range of 25−800 °C under the dry nitrogen atmosphere.

Electrochemical impedance spectroscopy (EIS) tests were carried out over the frequency range from 0.01 Hz to 100 kHz at amplitude of 10 mV using a potentio/galvanostat PARSTAT 2273 analyzer.

The ionic conductivity σ of all membranes was measured by means of EIS in a hermetic cell with stainless steel blocking electrodes. The ionic conductivities of the polymer electrolytes were calculated with the following equation:

$$\sigma = \frac{d}{R_{\rm b}S} \tag{1}$$

where σ is the ionic conductivity, $R_{\rm b}$ is the bulk resistance, d is the thickness of the polymer electrolyte, and S is the area of the stainless steel electrodes. The bulk resistance could be obtained from the impedance spectrum, and the thickness was gauged after the impedance tests.

Transference numbers in polymer electrolytes using Li/LiTFSI-PYR13TFSI-PMMA electrolyte/Li cell were determined by the method of Bruce *et al.* [19], which was a direct-current polarization method based on the d.c. polarization technique of Sorensen and Jacobsen [20]. The lithium ion transference number $t_{\rm Li^+}$ was calculated from the following equation:

$$t_{\rm Li^+} = \frac{I_{\rm s}(\Delta V - I_0 R_0)}{I_0(\Delta V - I_{\rm s}R_{\rm s})} \tag{2}$$

where ΔV is a constant d.c. bias voltage (0.01 V), I_0 is initial current (1.18 μA), $I_{\rm s}$ is steady-state current (0.692 μA), R_0 and R_s are sum of the charge transfer resistance and the passive membrane resistance of the initial and steady-state state, respectively. The fitting of the spectra was made using the non-linear least-squares fit method [20].

The cycling performance of Li/LiTFSI-PYR13TFSI-PMMA electrolyte/$LiFePO_4$ batteries was evaluated under charge/discharge rates of 0.1, 0.2, 0.5, and 1.0 C at 25 °C. The battery tests were performed using a Neware battery testing system (BTS-510A, ShenZhen,

DOI:10.1063/1674-0068/27/04/485-490

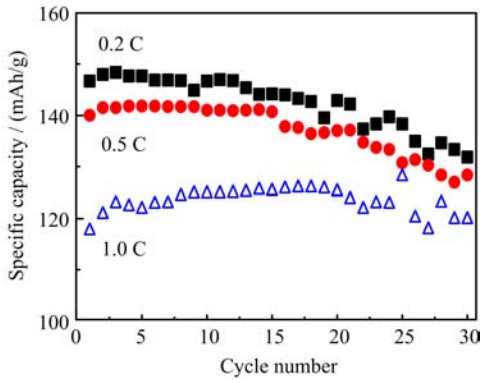

FIG. 1 Specific discharge capacity with cycle number for Li/LiTFSI-PYR13TFSI-PMMA electrolyte/$LiFePO_4$ at 0.2, 0.5, and 1.0 C, respectively.

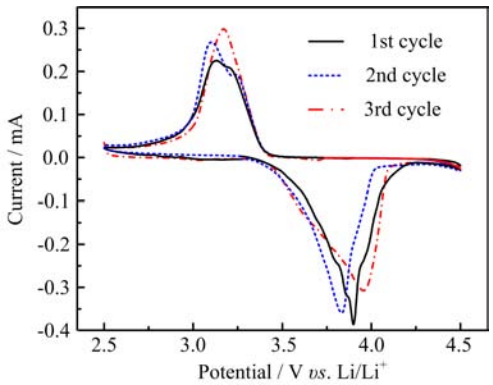

FIG. 2 Cyclic voltammetry of the Li/ILGPE/$LiFePO_4$ cell at scan rate of 0.1 mV/s.

China). The voltage cut-offs were fixed at 4.2 V (charge step) and 2.7 V (discharge step), respectively. The cyclic voltammetry measurements of a Li/LiTFSI-PYR13TFSI-PMMA electrolyte/$LiFePO_4$ cell were performed using CHI750B electrochemical work station over voltage range of 4.5 V to 2.5 V (*vs.* Li^+/Li) with a scan rate of 0.1 mV/s. All processes of cell assembling were performed in a dry Ar-filled glove box ($[H_2O]$<1 ppm).

III. RESULTS AND DISCUSSION

Figure 1 shows the discharge curves for the Li/LiTFSI-PYR13TFSI-PMMA electrolyte/$LiFePO_4$ at 0.2, 0.5, and 1.0 C. The cells with ILGPE show an initial discharge capacity of about 147 mAh/g at 0.2 C, 140 mAh/g at 0.5 C and 117 mAh/g at 1.0 C, respectively, and the cells retain 132 mAh/g at 0.2 C, 128 mAh/g at 0.5 C, and 120 mAh/g at 1.0 C after 30 cycles with charge-discharge efficiency of ca. 98% at every rate. The discharge capacity is not the highest for first few cycles due to the formation of "solid-electrolyte interphase" SEI layer. The layer acts as an interphase between the cathode $LiFePO_4$ and the electrolyte, and has the properties of a solid electrolyte with electronic resistivity. In the case of the rechargeable lithium battery, it is very important that there are uniform morphology and chemical composition for homogeneous current distribution.

Figure 2 presents cyclic voltammetry (CV) of the Li/ILGPE/$LiFePO_4$ cell at a scan rate of 0.1 mV/s. The cathodic and anodic peaks appear at 3.2 and 4.0 V on the first cycle, respectively. The smaller reduction currents are observed on the second and third sweep, which shows that the protective SEI membrane is not easily formed in the gel polymer electrolyte and at least needs three cycles. This result is consistent with the charge and discharge characteristics shown in Fig.1.

Figure 3 presents the surface images of the ionic liquid

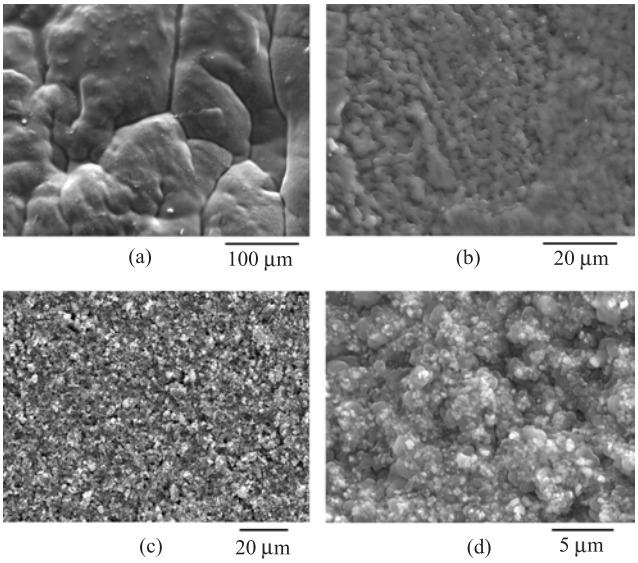

FIG. 3 SEM micrographs of ILGPE and $LiFePO_4$ electrodes before and after cycles. (a) Electrolyte before cycles, (b) electrolyte after cycles, (c) electrode before cycles, and (d) electrode after cycles.

gel polymer electrolyte and $LiFePO_4$ electrode before cycles and after cycles. There are a layer of membranes on the gel electrolyte and perfect shell membranes on the surface of active $LiFePO_4$ cluster. Such SEI layer is thick enough to prevent electron from tunneling electively and protect the electrolyte from further reduction. According to EIS (Fig.4) and Eq.(1) and Eq.(2), the ionic conductivity value is 4.29×10^{-4} S/cm and the lithium ion transference number is 0.44.

Figure 5 shows XPS wide scan spectrum of $LiFePO_4$ electrode surface before and after cycles. Compared with the fresh electrode, N and S element peaks appear after the cycles due to the SEI membrane composition on the electrode surface.

XPS high-resolution spectrum of nitrogen on the electrode after the cycles is shown in Fig.6. N1s peak at 398.7, 400.9, 401.3, and 402.1 eV can be attributed

DOI:10.1063/1674-0068/27/04/485-490

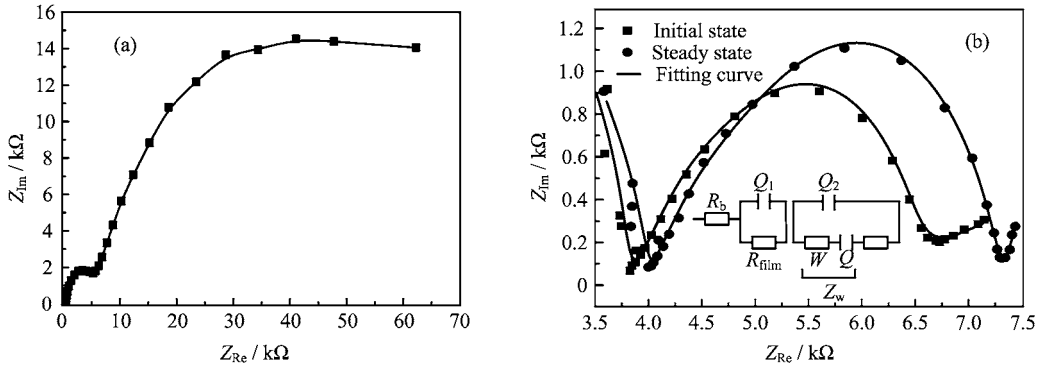

FIG. 4 Electrochemical impedance spectra of conductivity (a) and lithium ions transference number (b) measurement of the gel polymer electrolytes including PYR13TFSI at 25 °C. $R_{\rm film}$ is a passivating film resistance, Q_1 is a constant phase element in parallel, $R_{\rm ct}$ is a charge transfer resistance, W is the warburg impedance, and Q_2 is constant phase elements in parallel.

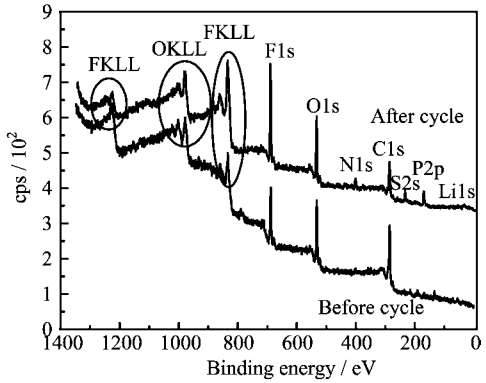

FIG. 5 XPS wide scan spectra of $LiFePO_4$ electrode surface before and after cycles. N and S photoelectron signals are observed in the spectrum.

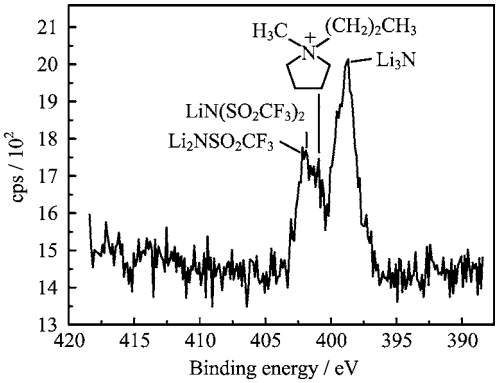

FIG. 6 XPS high-resolution spectrum of N1s on the electrode after cycles.

to Li_3N, $PYR13^+$, $Li_2NSO_2CF_3$, and $LiN(SO_2CF_3)_2$, respectively. When the ionic liquid gel polymer electrolyte contacts with the $LiFePO_4$ electrode, the PYR13TFSI diffuses to the surface of the electrode. During the cycles, the reaction of $N(SO_2CF_3)_3^-$ with Li^+ by obtaining the electrons maybe take place as shown in Fig.7 [23].

From the XPS high-resolution spectrum of carbon before cycles (Fig.8(a)), it can be seen that the main C1s peak at about 284.6 eV is ascribed to alkyl groups, and the peak at 290.6 eV corresponds to $-CF_2-$ in PVDF. After charge-discharge cycles, the number of C1s peaks in Fig.8(b) increases, that is, the peaks at 287.9 and 288.5 eV relate to C=O and O=C−O− group of Li−O−$COCCH_3CH_2$ [24], the peak at 289.1 eV corresponds to −C−F− in $C_2F_xLi_y$, and the peak at 292.3 eV is assigned to $-CF_3$ in $-N(SO_2CF_3)_2$. When the MMA is polymerized, a little unplolymerized MMA monomer is residual in the electrolyte, which can be found from TG curve shown in Fig.9. The MMA which accounts for 1.5% of electrolyte membrane total weight is volatile at the boiling point of 102 °C according to

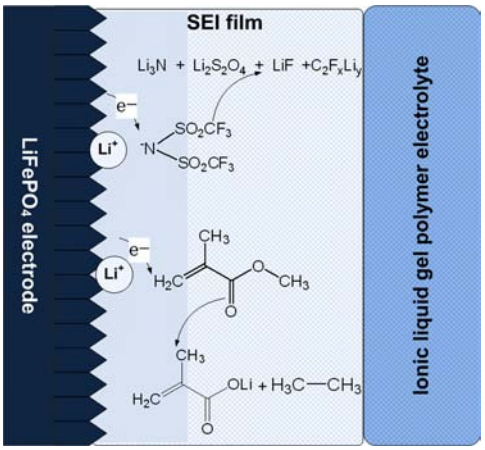

FIG. 7 An illustration of the surface membrane on $LiFePO_4$ electrode.

the TG curve. The reduction of electrolyte membrane including a little part of unpolymerized MMA monomer happens by electron transport through the surface layer, and thereby, follow-up reaction processes (Fig.7) appear between $LiFePO_4$ electrode surface and the elec-

DOI:10.1063/1674-0068/27/04/485-490

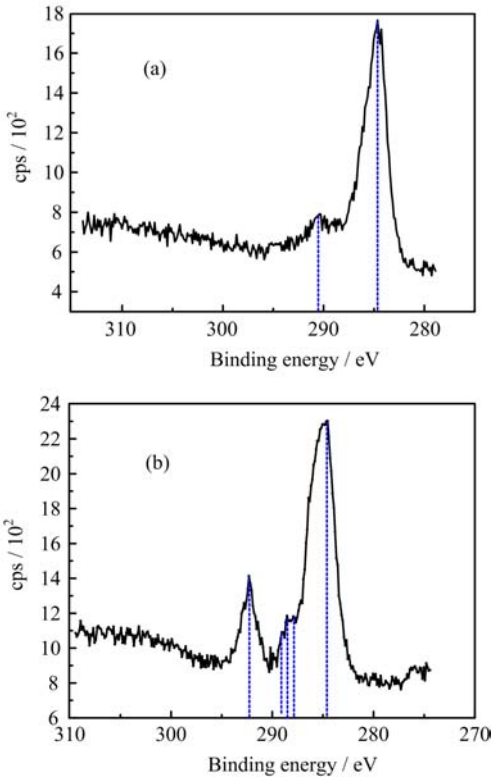

FIG. 8 XPS high-resolution spectra of C1s on the electrode before (a) and after (b) cycles.

trolyte surface. Therefore, the basal SEI (Fig.7) contains much more reduced productions of $TFSI^-$ and MMA. As the surface membrane becomes sufficiently thick, it blocks further electron transfer, and the system may approach steady state. In any event, the electrode-SEI membrane-electrolyte interface is very dynamic. Some electron tunneling may take place at certain locations of local, high electrical conductivity, and hence, small-scale reduction of gel electrolyte species continues. There is also dissolution-precipitation of species and secondary reactions between the electrode surface species and electrolyte surface species. Thus, the electrolyte side of the surface membranes is expected to be porous as shown in Fig.3(b), while the inner part, close to the electrode, is compact.

IV. CONCLUSION

Interface status of $LiFePO_4$ electrode and ionic liquid gel polymer electrolyte is analyzed and the performances of the cells are tested. The discharge capacity is not the highest for first few cycles due to the formation of "solid-electrolyte interphase" SEI layer. The protective SEI membrane is not easily formed in the gel polymer electrolyte and at least needs three cycles. N and S element peaks appear after the cycles due to reduced productions of TFSI- and MMA on the

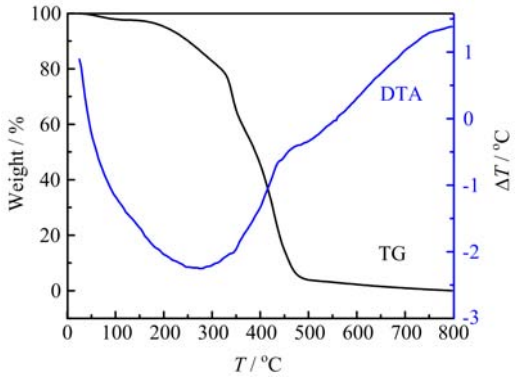

FIG. 9 TG-DTA thermograms of ILGPE in nitrogen flow.

electrode surface, that is, the SEI membrane composition. The cells with ILGPE show an initial discharge capacity of about 147 mAh/g at 0.2 C, 140 mAh/g at 0.5 C and 117 mAh/g at 1.0 C, respectively, and the cells retain 132 mAh/g at 0.2 C, 128 mAh/g at 0.5 C and 120 mAh/g at 1.0 C after 30 cycles with charge-discharge efficiency of ca. 98% at every rate. The ionic conductivity value is 4.29×10^{-4} S/cm and the lithium ion transference number is 0.44. The SEI formation process of electrode-electrolyte solid-solid interfaces endows gel batteries with the higher capacity and lithium ionic conductivity.

V. ACKNOWLEDGMENTS

This work was supported by the Innovative Research Team of green chemical technology in University of Heilongjiang Province, the Natural Science Foundation of Heilongjiang Province of China (No.B201007 and No.E201141), Harbin Innovation Talents of Science and Technology of Special Fund Project (No.2012RFQXG085), and Educational Commission of Heilongjiang Province of China (No.12521z008 and No.12511443).

[1] J. H. Lee, G. S. Kim, Y. M. Choi, W. I. Park, J. A. Rogers, and U. Paik, J. Power Sources **184**, 308 (2008).
[2] D. Chen, S. Indris, M. Schulz, B. Gamer, and R. Mönig, J. Power Sources **196**, 6382 (2011).
[3] T. Ishihara, Y. Yokoyama, F. Kozono, and H. Hayashi, J. Power Sources **196**, 6956 (2011).
[4] F. Croce, A. Epifanio, J. Hassoun, P. Reale, and B. Scrosati, J. Power Sources **119**, 399 (2003).
[5] J. H. Shin, W. A. Henderson, G. B.Appetecchi, F. Alessandrini, and S. Passerini, Electrochim. Acta **50**, 3859 (2005).
[6] G. T. Kim, G. B. Appetecchi, F. Alessandrini, and S. Passerini, J. Power Sources **171**, 861 (2007).

DOI:10.1063/1674-0068/27/04/485-490

[7] L. T. Costa, L. J. A. Siqueira, B. G. Nicolau, and M. C. C. Ribeiro, Vib. Spectrosc. **54**, 155 (2010).
[8] Y. Yoshida, O. Baba, and G. Saito, J. Phys. Chem. B 111, 4742 (2007).
[9] H. Sano, H. Sakaebe, and H. Matsumoto, J. Power Sources **196**, 6663 (2011).
[10] G. T. Kim, S. S. Jeong, M. Z. Xue, A. Balducci, M. Winter, S. Passerini, F. Alessandrini, and G. B. Appetecchi, J. Power Sources **199**, 239 (2012).
[11] A. Noda and M. Watanabe, Electrochim. Acta **45**, 1265 (2000).
[12] J. Fuller, A. C. Breda, and R. T. Carlin, J. Electroanal. Chem. **459**, 29 (1998).
[13] K. S. Kim, S. Y. Park, S. Choi, and H. Lee, J. Power Sources **155**, 385 (2006).
[14] D. Bansal, F. Cassel, F. Croce, M. Hendrickson, E. Plichta, and M. Salomon, J. Phys. Chem. B **109**, 4492 (2005).
[15] J. H. Shin, W. A. Henderson, C. Tizzani, S. Passerini, S. S. Jeong, and K. W. Kim, J. Electrochem. Soc. **153**, A1649 (2006).
[16] B. Singh and S. Sekhon, J. Phys. Chem. B **109**, 16539 (2005).
[17] J. H. Shin, W. A. Henderson, and S. Passerini, J. Electrochem. Soc. **152**, A978 (2005).
[18] H. Cheng, C. Zhu, B. Huang, M. Lu, and Y. Yang, Electrochim. Acta **52**, 5789 (2007).
[19] A. Hayashi, Y. Nishio, H. Kitaura, and M. Tatsumisago, Electrochem. Commun. **10**, 1860 (2008).
[20] P. G. Bruce and C. A. Vincent, J. Electroanal. Chem. **225**, 1 (1987).
[21] P. R. Sorensen and T. Jacobsen, Electrochim. Acta **27**, 1671 (1982).
[22] G. B. Appetecchi, G. T. Kim, M. Montanino, M. Carewska, R. Marcilla, D. Mecerreyes, and I. D. Meatza, J. Power Sources **195**, 3668 (2010).
[23] D. Aurbach, I. Weissman, A. Schechter, and H. Cohen, Langmuir **12**, 3991 (1996).
[24] D. Bar-Tow, E. Peled, and L. Burstein, J. Electrochem. Soc. **146**, 824 (1999).

DOI:10.1063/1674-0068/27/04/485-490